molecular pharmaceutics

Article

Cite This: Mol. Pharmaceutics XXXX, XXX, XXX−XXX

pubs.acs.org/molecularpharmaceutics

Characterization of Novel ^{18}F-Labeled Phenoxymethylpyridine Derivatives as Amylin Imaging Probes

Hiroyuki Watanabe,[†] Masashi Yoshimura,[†] Kohei Sano,[‡] Yoichi Shimizu,[‡] Sho Kaide,[†] Yuji Nakamoto,[§] Kaori Togashi,[§] Masahiro Ono,*[,†] and Hideo Saji[†]

[†]Department of Patho-Functional Bioanalysis, Graduate School of Pharmaceutical Sciences, Kyoto University, 46-29 Yoshida Shimoadachi-cho, Sakyo-ku, Kyoto 606-8501, Japan

[‡]Division of Clinical Radiology Service, Kyoto University Hospital, 54 Shogoin Kawahara-cho, Sakyo-ku, Kyoto 606-8507, Japan

[§]Department of Diagnostic Imaging and Nuclear Medicine, Graduate School of Medicine, Kyoto University, 54 Shogoin Kawahara-cho, Sakyo-ku, Kyoto 606-8507, Japan

Supporting Information

ABSTRACT: Deposition of islet amyloid consisting of amylin constitutes one of pathological hallmarks of type 2 diabetes mellitus (T2DM), and it may be involved in the development and progression of T2DM. However, the details about the relationship between the deposition of islet amyloid and the pathology of T2DM remain unclear, since no useful imaging tracer enabling the visualization of pancreatic amylin is available. In the present study, we synthesized and evaluated six novel ^{18}F-labeled phenoxymethylpyridine (PMP) derivatives as amylin imaging probes. All ^{18}F-labeled PMP derivatives showed not only affinity for islet amyloid in the post-mortem T2DM pancreatic sections but also excellent pharmacokinetics in normal mice. Furthermore, ex vivo autoradiographic studies demonstrated that [^{18}F]FPMP-5 showed intense labeling of islet amyloids in the diabetes model mouse pancreas in vivo. The preclinical studies suggested that [^{18}F]FPMP-5 may have potential as an imaging probe that targets amylin aggregates in the T2DM pancreas.

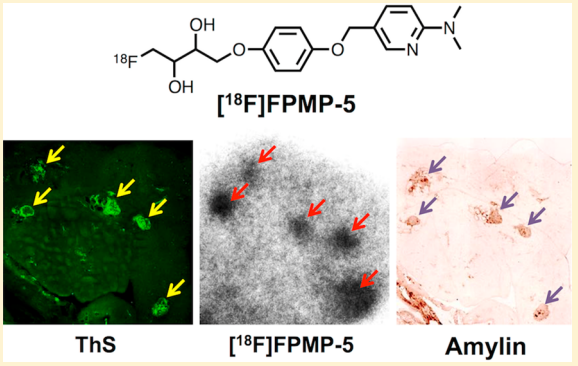

KEYWORDS: *amylin, imaging, type 2 diabetes, fluorine-18*

INTRODUCTION

Diabetes mellitus is classified as metabolic disorders characterized by hyperglycemia due to defects in insulin secretion, insulin action, or both.[1] The chronic hyperglycemia of diabetes mellitus induces metabolic failure of major nutrients, such as fat and protein.[1] Moreover, diabetes mellitus is associated with a number of complications, namely, diabetic nephropathy, diabetic retinopathy, and diabetic neuropathy.[1] These diabetic complications not only greatly reduce the quality-of-life of diabetes patients, but also shorten their lifespan. Recent research revealed that adults with diabetes died 4.6 years earlier than adults without diabetes.[2] The World Health Organization stated that the number of people with diabetes had risen markedly and there were approximately 422 million diabetes patients worldwide in 2014, which equates to 8.5% of the adult population.[3] Due to population aging, rapid urbanization, and changes in dietary habits, the number of people suffering from diabetes is still increasing throughout the world. The International Diabetes Federation produced estimates of diabetes prevalence in 2013, on the basis of which the number is expected to rise to 592 million by 2035.[4] According to its cause, diabetes mellitus is classified into four categories, type 1, type 2, other types, and gestational diabetes mellitus.[1] Among them, type 2 diabetes mellitus (T2DM) is the most common form of diabetes, accounting for 90−95% of people with diabetes mellitus.[1] The current diagnosis of T2DM is based on the blood glucose level and glucose tolerance.[5−7] However, this method is unable to detect T2DM in the early stage.[8] Since T2DM is known to be a progressive disease, the therapeutic intervention in the early phase is important. Therefore, the development of a novel method for the early diagnosis of T2DM is strongly expected.

The gradual and progressive loss of the β-cell mass (BCM) is believed to be a characteristic of T2DM.[9−11] Some reports state that BCM in T2DM patients is reduced to less than 50% of that of healthy controls.[11] Therefore, a number of radioactive agents for in vivo imaging of pancreatic β-cells have been developed for the purpose of improving understanding of the pathophysiology of T2DM.[12−15] In the future, β-cell imaging may be used as a critical tool for understanding the progression of T2DM. However, it is considered that the

Received: July 16, 2018
Revised: October 9, 2018
Accepted: October 29, 2018

DOI: 10.1021/acs.molpharmaceut.8b00756
Mol. Pharmaceutics XXXX, XXX, XXX−XXX

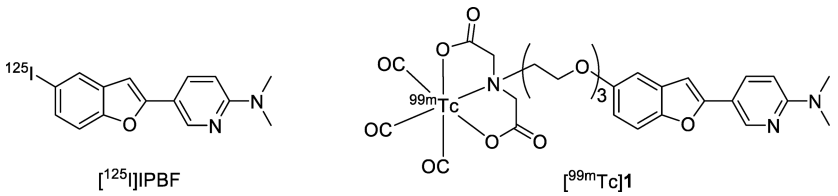

Figure 1. Chemical structures of [^{125}I]IPBF and [^{99m}Tc]**1**.

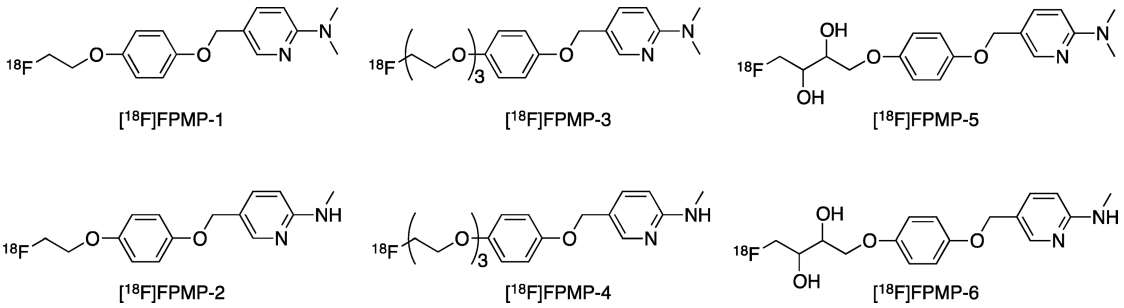

Figure 2. Chemical structures of ^{18}F-labeled PMP derivatives.

proliferation of β-cells and insulin secretion are promoted in order to compensate for insulin resistance in the early phase of T2DM,[16,17] which means that the BCM may not decrease monotonically. Previous research using rodent models reported that BCM expansion was observed under insulin-resistant conditions.[18] From the above, we considered that it is difficult to diagnose T2DM in the early phase solely based on β-cell imaging.

Islet amyloid deposits are one of the characteristic pathologic features of the T2DM pancreas.[19] Islet amyloid mainly forms by the aggregation of amylin, also known as islet amyloid polypeptide (IAPP) consisting of a 37-amino acid peptide.[20] Amylin is a neuroendocrine peptide hormone that is coproduced and cosecreted along with insulin from pancreatic β-cells.[20] The aggregation of amylin peptide has been suggested to occur in a stepwise process. Monomeric amylin peptide forms amyloid fibrils via soluble oligomers and protofibrils, some of which are toxic to the pancreatic β-cells.[20] In addition, the amount of islet amyloid formation has been reported to be correlated with a BCM reduction.[21] Since islet amyloid depositions are found in up to 90% of T2DM patients at autopsy, it may be common to the T2DM pathology.[19] Taken together, islet amyloid deposition may be involved in the pathogenesis of T2DM. Despite its potential importance, the lack of a method for visualizing amyloid depositions in the T2DM pancreas makes it difficult to conduct research on islet amyloid in vivo. Therefore, the development of a radiotracer for amylin imaging may facilitate intensive research focusing on the pathogenesis of T2DM.

We previously found out that the Aβ imaging probe, ^{125}I-labeled pyridyl benzofuran (PBF), has the potential to serve as an amylin imaging probe.[22] More recently, other groups reported that two Aβ imaging probes, [^{18}F]FDDNP and [^{18}F]florbetapir, showed the feasibility for amylin imaging.[23,24] However, the pharmacokinetics of these probes in pancreas and its surrounding organs is not suitable for in vivo imaging of amylin. We also reported that ^{99m}Tc-labeled PBF derivatives meet the fundamental requirements for radioactive amylin imaging probes (Figure 1).[25] In particular, [^{99m}Tc]**1** showed specific binding to amylin aggregates transplanted into the pancreas of a living mouse.[25] However, [^{99m}Tc]**1** displayed a low initial uptake by the pancreas of the normal mouse, whereas it showed intensive accumulation in the liver.[25] For in vivo amylin imaging, a low initial uptake of an imaging probe by the pancreas weakens the on-target signal; on the other hand, a high accumulation in the liver leads to the noise signal. Therefore, structural modification based on [^{99m}Tc]**1** may be essential in order to improve the pharmacokinetics. Herein, we describe a series of phenoxymethylpyridine (PMP) derivatives, with a structure simpler than PBF as a binding moiety. Recently, benzyloxybenzene, whose chemical structure is similar to PMP, was reported to be a promising scaffold for imaging agents targeting β-amyloid (Aβ) plaques.[26−28] In addition, our previous research revealed the feasibility of amylin imaging with Aβ imaging probes.[22] Taken together, we hypothesized that PMP derivatives have the potential to act as amylin imaging probes. The iminodiacetic acid (IDA) core, the ^{99m}Tc-chelating moiety of [^{99m}Tc]**1**, is sometimes prone to accumulation in the liver.[29,30] Instead of ^{99m}Tc, we introduce ^{18}F into PMP derivatives via variable hydrophilic linkers. Considering the above, we designed, synthesized, and evaluated six novel PMP derivatives as amylin imaging probes (Figure 2). In our previous study, ex vivo experiments with islet amyloid model mice established by the orthotopic implantation method were carried out in order to determine the in vivo binding affinity of ligands.[25] These model mice were suitable for the screening of amylin imaging probes in vivo; however, they probably do not show symptoms of diabetes. In this study, we conducted ex vivo experiments using obese transgenic mice, which express human amylin peptides and develop an islet pathology resembling that in humans with T2DM.[31,32] Therefore, the present study shows PMP derivatives' binding affinity in vivo for islet amyloids, which was evaluated under conditions close to those of the living T2DM pancreas.

EXPERIMENTAL SECTION

General Remarks. All reagents were commercial products and used without further purification unless indicated otherwise. W-Prep 2XY (Yamazen Corporation, Osaka, Japan) was used for silica gel column chromatography on a

DOI: 10.1021/acs.molpharmaceut.8b00756
Mol. Pharmaceutics XXXX, XXX, XXX−XXX

Hi Flash silica gel column (40 μm, 60 Å, Yamazen) or Hi Flash aminopropyl silica gel column (40 μm, 60 Å, Yamazen). LC-20AD (Shimadzu Corporation, Kyoto, Japan) equipped with an SPD-20A UV detector (Shimadzu) was used for high-performance liquid chromatography (HPLC). LC-9101 (Japan Analytical Industry, Tokyo, Japan) with a JAIGEL-2H column and $CHCl_3$ as the mobile phase was used for recycling preparative HPLC. ^{1}H NMR spectra were recorded using a JEOL JNM-ECS400 or JEOL ECA-500 spectrometer, and chemical shifts are reported in δ (ppm) relative to TMS as an internal standard. Coupling constants are reported in Hertz. Multiplicity was defined as singlet (s), doublet (d), triplet (t), or multiplet (m). Low-resolution mass spectra (LRMS) were obtained using a SHIMADZU LCMS-2020. High-resolution mass spectrometry (HRMS) was conducted with a JEOL JMS-700.

Chemistry. *Methyl 6-(dimethylamino)nicotinate (**1**).* To a solution of methyl 6-aminonicotinate (1.52 g, 10 mmol) in acetic acid (40 mL) was added paraformaldehyde (3.0 g, 100 mmol) and $NaBH_3CN$ (1.88 g, 30 mmol). The reaction mixture was stirred at room temperature for 23 h and then quenched with 2 N NaOH aq. The solution was extracted with AcOEt (100 mL × 2). The organic layers were combined and dried over Na_2SO_4. Evaporation of the solvent afforded a residue, which was purified by silica gel chromatography (AcOEt/hexane = 1/3) to give 1.54 g of **1** (85.5%). ^{1}H NMR (400 MHz, $CDCl_3$, δ): 8.80 (d, J = 2.3 Hz, 1H), 8.00 (dd, J = 9.0, 2.0 Hz, 1H), 6.47 (d, J = 9.2 Hz, 1H), 3.86 (s, 3H), 3.17 (s, 6H). MS (ESI) (m/z): 181 [MH^+].

*(6-(Dimethylamino)pyridin-3-yl)methanol (**2**).* A solution of **1** (1.56 g, 8.63 mmol) in THF (20 mL) was added dropwisely to a stirred suspension of lithium aluminum hydride (655 mg, 17.3 mmol) in THF (20 mL) at −78 °C. The reaction mixture was stirred at −78 °C for 4.5 h and then at 0 °C for 1 h. Water (3 mL), 2 N NaOH (3 mL), and water (3 mL) were added successively at 0 °C, and the resulting mixture was stirred vigorously. The mixture was then filtered through Celite. The filtrate was extracted with AcOEt (70 mL × 2), and the organic layers were combined and dried over Na_2SO_4. Evaporation of the solvent afforded a residue, which was purified by silica gel chromatography (AcOEt/hexane = 5/1) to give 1.02 g of **2** (77.4%). ^{1}H NMR (500 MHz, $CDCl_3$, δ): 8.10 (d, J = 2.3 Hz, 1H), 7.50 (dd, J = 8.6, 2.3 Hz, 1H), 6.51 (d, J = 8.8 Hz, 1H), 4.53 (s, 2H), 3.09 (s, 6H), 1.70 (s, 1H). MS (ESI) (m/z): 153 [MH^+].

*Methyl 6-(methylamino)nicotinate (**3**).* To a solution of methyl 6-chloronicotinate (2.0 g, 11.7 mmol) in DMF (20 mL) was added methylamine (30% in MeOH, 4 mL). The reaction mixture was stirred at 50 °C for 19 h. The solution was allowed to cool to room temperature and then extracted with AcOEt (70 mL × 2). The organic layers were combined and dried over Na_2SO_4. Evaporation of the solvent afforded a residue, which was purified by silica gel chromatography (AcOEt/hexane = 1/1) to give 764 mg of **3** (39.4%). ^{1}H NMR (400 MHz, $CDCl_3$, δ): 8.75 (d, J = 2.0 Hz, 1H), 8.01 (dd, J = 8.8, 2.0 Hz, 1H), 6.36 (d, J = 9.2 Hz, 1H), 5.05 (s, 1H), 3.87 (s, 3H), 2.99 (d, J = 5.2 Hz, 3H). MS (ESI) (m/z): 167 [MH^+].

*(6-(Methylamino)pyridin-3-yl)methanol (**4**).* A solution of **3** (764 mg, 4.60 mmol) in THF (15 mL) was added dropwisely to a stirred suspension of lithium aluminum hydride (349 mg, 9.20 mmol) in THF (15 mL) at −78 °C. The reaction mixture was stirred at −78 °C for 3 h and then at 0 °C for 2 h. Water (3 mL), 2 N NaOH (3 mL), and water (3 mL) were added successively at 0 °C, and the resulting mixture was stirred vigorously. The mixture was then filtered through Celite. The filtrate was extracted with AcOEt (70 mL × 2), and the organic layers were combined and dried over Na_2SO_4. Evaporation of the solvent afforded a residue, which was purified by silica gel chromatography ($CHCl_3$/MeOH = 10/1) to give 355 mg of **4** (55.9%). ^{1}H NMR (400 MHz, $CDCl_3$, δ): 8.01 (d, J = 2.4 Hz, 1H), 7.50 (dd, J = 8.4, 2.4 Hz, 1H), 6.39 (d, J = 8.4 Hz, 1H), 4.59 (s, 1H), 4.53 (s, 2H), 2.91 (d, J = 5.2 Hz, 3H), 1.94 (s, 1H). MS (ESI) (m/z): 139 [MH^+].

*2-(4-((6-(Dimethylamino)pyridin-3-yl)methoxy)phenoxy)-ethyl 4-methylbenzenesulfonate (**5**).* 2-(4-Hydroxyphenoxy)-ethyl 4-methylbenzenesulfonate was prepared according to ref 28. To a solution of **2** (152 mg, 1 mmol) and 2-(4-hydroxyphenoxy)ethyl 4-methylbenzenesulfonate (308.4 mg, 1 mmol) in THF (10 mL) was added triphenylphosphine (393.4 mg, 1.5 mmol), and then the mixture was cooled to 0 °C. Diisopropyl azodicarboxylate (303.3 mg, 1.5 mmol) in THF (5 mL) was added dropwisely at 0 °C, and then the reaction mixture was stirred at room temperature for 8.5 h. To the solution, triphenylphosphine (78.7 mg, 0.3 mmol) and diisopropyl azodicarboxylate (60.7 mg, 0.3 mmol) were added, and then the solution was stirred at room temperature for 18.5 h. Evaporation of the solvent afforded a residue, which was purified by silica gel chromatography (AcOEt/hexane = 1/1) to give 121 mg of **5** (27.3%). ^{1}H NMR (400 MHz, $CDCl_3$, δ): 8.17 (d, J = 2.4 Hz, 1H), 7.82 (d, J = 8.4 Hz, 2H), 7.51 (dd, J = 8.8, 2.4 Hz, 1H), 7.34 (d, J = 8.4 Hz, 2H), 6.85 (d, J = 9.2 Hz, 2H), 6.71 (d, J = 8.8 Hz, 2H), 6.53 (d, J = 9.2 Hz, 1H), 4.84 (s, 2H), 4.34 (t, J = 4.8 Hz, 2H), 4.09 (t, J = 4.8 Hz, 2H), 3.09 (s, 6H), 2.45 (s, 3H). MS (ESI) (m/z): 443 [MH^+].

*2-(4-((6-(Methylamino)pyridin-3-yl)methoxy)phenoxy)-ethyl 4-methylbenzenesulfonate (**6**).* To a solution of **4** (138.2 mg, 1 mmol) and 2-(4-hydroxyphenoxy)ethyl 4-methylbenzenesulfonate (277.5 mg, 0.9 mmol) in THF (6 mL) was added triphenylphosphine (524.6 mg, 2 mmol), and then the mixture was cooled to 0 °C. Diisopropyl azodicarboxylate (404.4 mg, 2 mmol) in THF (3 mL) was added dropwisely at 0 °C, and then the reaction mixture was stirred at room temperature for 5 h. Evaporation of the solvent afforded a residue, which was purified by silica gel chromatography (AcOEt/hexane = 3/1) and recycling preparative HPLC with $CHCl_3$ to give 83.5 mg of **6** (21.6%). ^{1}H NMR (400 MHz, $CDCl_3$, δ): 8.10 (d, J = 2.4 Hz, 1H), 7.81 (d, J = 8.4 Hz, 2H), 7.53 (dd, J = 8.4, 2.4 Hz, 1H), 7.34 (d, J = 8.0 Hz, 2H), 6.85 (d, J = 9.2 Hz, 2H), 6.72 (d, J = 9.2 Hz, 2H), 6.43 (d, J = 8.4 Hz, 1H), 4.84 (s, 2H), 4.79 (s, 1H), 4.34 (t, J = 4.8 Hz, 2H), 4.10 (t, J = 4.8 Hz, 2H), 2.93 (d, J = 4.8 Hz, 3H), 2.45 (s, 3H). MS (ESI) (m/z): 429 [MH^+].

*2-(2-(2-(4-((6-(Dimethylamino)pyridin-3-yl)methoxy)-phenoxy)ethoxy)ethoxy)ethyl 4-methylbenzenesulfonate (**7**).* 2-(2-(2-(4-Hydroxyphenoxy)ethoxy)ethoxy)ethyl 4-methylbenzenesulfonate was prepared according to ref 28. To a solution of **2** (152.2 mg, 1 mmol) and 2-(2-(2-(4-hydroxyphenoxy)ethoxy)ethoxy)ethyl 4-methylbenzenesulfonate (396.5 mg, 1 mmol) in THF (6 mL) was added triphenylphosphine (393.4 mg, 1.5 mmol), and then the mixture was cooled to 0 °C. Diisopropyl azodicarboxylate (303.3 mg, 1.5 mmol) in THF (2 mL) was added dropwisely at 0 °C, and then the reaction mixture was stirred at room temperature for 20 h. Evaporation of the solvent afforded a

DOI: 10.1021/acs.molpharmaceut.8b00756
Mol. Pharmaceutics XXXX, XXX, XXX−XXX

residue, which was purified by silica gel chromatography (AcOEt/hexane = 3/1) to give 279.1 mg of **7** (52.6%). ^{1}H NMR (500 MHz, $CDCl_3$, δ): 8.18 (d, J = 2.5 Hz, 1H), 7.80 (d, J = 8.5 Hz, 2H), 7.53 (dd, J = 8.5, 2.5 Hz, 1H), 7.33 (d, J = 8.5 Hz, 2H), 6.88 (d, J = 9.0 Hz, 2H), 6.83 (d, J = 9.0 Hz, 2H), 6.53 (d, J = 8.5 Hz, 1H), 4.85 (s, 2H), 4.16 (t, J = 5.0 Hz, 2H), 4.06 (t, J = 4.5 Hz, 2H), 3.79 (t, J = 5.5 Hz, 2H), 3.70 (t, J = 5.0 Hz, 2H), 3.67−3.60 (m, 4H), 3.09 (s, 6H), 2.43 (s, 3H). MS (ESI) (m/z): 531 [MH^+].

*2-(2-(2-(4-((6-(Methylamino)pyridin-3-yl)methoxy)-phenoxy)ethoxy)ethoxy)ethyl 4-methylbenzenesulfonate (**8**).* To a solution of **4** (138.2 mg, 1 mmol) and 2-(2-(2-(4-hydroxyphenoxy)ethoxy)ethoxy)ethyl 4-methylbenzenesulfonate (396.5 mg, 1 mmol) in THF (6 mL) was added triphenylphosphine (393.4 mg, 1.5 mmol), and then the mixture was cooled to 0 °C. Diisopropyl azodicarboxylate (303.3 mg, 1.5 mmol) in THF (2 mL) was added dropwisely at 0 °C, and then the reaction mixture was stirred at room temperature for 17 h. Evaporation of the solvent afforded a residue, which was purified by silica gel chromatography (AcOEt/hexane = 3/1) to give 115.1 mg of **8** (22.3%). ^{1}H NMR (500 MHz, $CDCl_3$, δ): 8.11 (d, J = 2.0 Hz, 1H), 7.80 (d, J = 8.0 Hz, 2H), 7.53 (d, J = 8.5 Hz, 1H), 7.33 (d, J = 8.0 Hz, 2H), 6.88 (d, J = 9.0 Hz, 2H), 6.84 (d, J = 8.5 Hz, 2H), 6.42 (d, J = 8.5 Hz, 1H), 4.85 (s, 2H), 4.68 (s, 1H), 4.16 (t, J = 4.5 Hz, 2H), 4.06 (t, J = 4.5 Hz, 2H), 3.80 (t, J = 5.0 Hz, 2H), 3.70 (t, J = 5.0 Hz, 2H), 3.66−3.60 (m, 4H), 2.93 (d, J = 5.5 Hz, 3H), 2.43 (s, 3H). MS (ESI) (m/z): 517 [MH^+].

*5-((4-(2-Fluoroethoxy)phenoxy)methyl)-N,N-dimethylpyridin-2-amine (**9**: FPMP-1).* To a solution of **5** (88.5 mg, 0.2 mmol) in THF (7 mL) was added TBAF solution (1 M in THF, 0.64 mL). The reaction mixture was refluxed for 2 h. The solution was allowed to cool to room temperature and then extracted with AcOEt (70 mL × 2). The organic layers were combined and dried over Na_2SO_4. Evaporation of the solvent afforded a residue, which was purified by silica gel chromatography (AcOEt/hexane = 1/1) to give 30.0 mg of **9** (51.6%). ^{1}H NMR (500 MHz, $CDCl_3$, δ): 8.18 (d, J = 2.5 Hz, 1H), 7.52 (dd, J = 9.0, 2.5 Hz, 1H), 6.91−6.85 (m, 4H), 6.53 (d, J = 9.0 Hz, 1H), 4.86 (s, 2H), 4.79−4.68 (m, 2H), 4.20−4.13 (m, 2H), 3.09 (s, 6H). HRMS (FAB+) (m/z): [MH^+] calcd for $C_{16}H_{20}FN_2O_2$, 291.1509; found, 291.1506.

*5-((4-(2-Fluoroethoxy)phenoxy)methyl)-N-methylpyridin-2-amine (**10**: FPMP-2).* To a solution of **6** (68.6 mg, 0.16 mmol) in THF (6 mL) was added TBAF solution (1 M in THF, 0.64 mL). The reaction mixture was refluxed for 2 h. The solution was allowed to cool to room temperature and then extracted with AcOEt (60 mL × 2). The organic layers were combined and dried over Na_2SO_4. Evaporation of the solvent afforded a residue, which was purified by silica gel chromatography (AcOEt/hexane = 3/1) to give 33.2 mg of **10** (75.1%). ^{1}H NMR (400 MHz, $CDCl_3$, δ): 8.12 (d, J = 2.4 Hz, 1H), 7.52 (dd, J = 8.4, 2.4 Hz, 1H), 6.91−6.85 (m, 4H), 6.41 (d, J = 8.8 Hz, 1H), 4.85 (s, 2H), 4.81−4.67 (m, 2H), 4.57 (s, 1H), 4.21−4.12 (m, 2H), 2.93 (d, J = 5.2 Hz, 3H). HRMS (FAB+) (m/z): [MH^+] calcd for $C_{15}H_{18}FN_2O_2$, 277.1352; found, 277.1359.

*5-((4-(2-(2-(2-Fluoroethoxy)ethoxy)ethoxy)phenoxy)-methyl)-N,N-dimethylpyridin-2-amine (**11**: FPMP-3).* To a solution of **7** (159.2 mg, 0.3 mmol) in THF (6 mL) was added TBAF solution (1 M in THF, 1.2 mL). The reaction mixture was refluxed for 2 h. The solution was allowed to cool to room temperature and then extracted with AcOEt (70 mL × 2). The organic layers were combined and dried over Na_2SO_4. Evaporation of the solvent afforded a residue, which was purified by silica gel chromatography (AcOEt/hexane = 3/1) to give 67.8 mg of **11** (59.7%). ^{1}H NMR (500 MHz, $CDCl_3$, δ): 8.18 (d, J = 2.0 Hz, 1H), 7.52 (dd, J = 9.0, 2.5 Hz, 1H), 6.89−6.83 (m, 4H), 6.53 (d, J = 9.0 Hz, 1H), 4.85 (s, 2H), 4.62−4.51 (m, 2H), 4.09 (t, J = 4.5 Hz, 2H), 3.84 (t, J = 4.5 Hz, 2H), 3.80−3.71 (m, 6H), 3.09 (s, 6H). HRMS (FAB+) (m/z): [MH^+] calcd for $C_{20}H_{28}FN_2O_4$, 379.2033; found, 379.2043.

*5-((4-(2-(2-(2-Fluoroethoxy)ethoxy)ethoxy)phenoxy)-methyl)-N-methylpyridin-2-amine (**12**: FPMP-4).* To a solution of **8** (87.8 mg, 0.17 mmol) in THF (6 mL) was added TBAF solution (1 M in THF, 0.68 mL). The reaction mixture was refluxed for 2.5 h. The solution was allowed to cool to room temperature and then extracted with AcOEt (60 mL × 2). The organic layers were combined and dried over Na_2SO_4. Evaporation of the solvent afforded a residue, which was purified by aminopropyl silica gel chromatography (AcOEt/hexane = 3/1) to give 39.7 mg of **12** (64.1%). ^{1}H NMR (400 MHz, $CDCl_3$, δ): 8.12 (d, J = 2.4 Hz, 1H), 7.52 (dd, J = 8.4, 2.0 Hz, 1H), 6.89−6.84 (m, 4H), 6.41 (d, J = 8.8 Hz, 1H), 4.85 (s, 2H), 4.64−4.50 (m, 3H), 4.09 (t, J = 4.8 Hz, 2H), 3.84 (t, J = 5.2 Hz, 2H), 3.81−3.70 (m, 6H), 2.93 (d, J = 5.2 Hz, 3H). HRMS (FAB+) (m/z): [MH^+] calcd for $C_{19}H_{26}FN_2O_4$, 365.1877; found, 365.1884.

*(5-(4-(Benzyloxy)phenoxy)-2,2-dimethyl-1,3-dioxolan-4-yl)methyl 4-methylbenzenesulfonate (**13**).* To a solution of methyl 4-(benzyloxy)phenol (1.0 g, 5 mmol) in DMF (10 mL) was added K_2CO_3 (1.38 g, 10 mmol) and (−)-1,4-di-O-tosyl-2,3-O-isopropylidene-L-threitol (2.82 g, 6 mmol). The reaction mixture was stirred at 70 °C for 21 h. The solution was allowed to cool to room temperature and then extracted with AcOEt (70 mL × 2). The organic layers were combined and dried over Na_2SO_4. Evaporation of the solvent afforded a residue, which was purified by silica gel chromatography (AcOEt/hexane = 1/5) to give 1.64 g of **13** (66.0%). ^{1}H NMR (400 MHz, $CDCl_3$, δ): 7.80 (d, J = 8.0 Hz, 2H), 7.44−7.31 (m, 6H), 6.89 (d, J = 9.2 Hz, 2H), 6.77 (d, J = 9.2 Hz, 2H), 5.02 (s, 2H), 4.26 (dd, J = 9.6, 3.2 Hz, 1H), 4.20−4.05 (m, 5H), 3.93 (dd, J = 9.6, 4.8 Hz, 1H), 2.43 (s, 3H), 1.41 (s, 3H), 1.38 (s, 3H). MS (APCI) (m/z): 499 [MH^+].

*(5-(4-Hydroxyphenoxy)-2,2-dimethyl-1,3-dioxolan-4-yl)-methyl 4-methylbenzenesulfonate (**14**).* To a solution of **13** (1.64 g, 3.29 mmol) in a mixture of MeOH (25 mL) and THF (10 mL) was added 10% Pd/C (150 mg). The reaction mixture was stirred vigorously for 7 h at 50 °C under an H_2 atmosphere. The reaction mixture was filtered through Celite, and then the filtrate was evaporated. The residue was purified by silica gel chromatography (AcOEt/hexane = 1/3) to give 1.01 g of **14** (75.2%). ^{1}H NMR (400 MHz, $CDCl_3$, δ): 7.80 (d, J = 8.0 Hz, 2H), 7.33 (d, J = 8.4 Hz, 2H), 6.78−6.72 (m, 4H), 4.54 (s, 1H), 4.26 (dd, J = 9.6, 3.2 Hz, 1H), 4.20−4.05 (m, 4H), 3.93 (dd, J = 9.2, 4.0 Hz, 1H), 2.44 (s, 3H), 1.41 (s, 3H), 1.38 (s, 3H). MS (APCI) (m/z): 409 [MH^+].

*(5-(4-((6-(Dimethylamino)pyridin-3-yl)methoxy)-phenoxy)-2,2-dimethyl-1,3-dioxolan-4-yl)methyl 4-methylbenzenesulfonate (**15**).* To a solution of **2** (152.2 mg, 1 mmol) and **14** (408.5 mg, 1 mmol) in THF (6 mL) was added triphenylphosphine (393.4 mg, 1.5 mmol), and then the mixture was cooled to 0 °C. Diisopropyl azodicarboxylate (303.3 mg, 1.5 mmol) in THF (3 mL) was added dropwisely at 0 °C, and then the reaction mixture was stirred at room

DOI: 10.1021/acs.molpharmaceut.8b00756
Mol. Pharmaceutics XXXX, XXX, XXX−XXX

temperature for 19 h. Evaporation of the solvent afforded a residue, which was purified by silica gel chromatography (AcOEt/hexane = 1/1) to give 339.5 mg of **15** (62.6%). ^{1}H NMR (400 MHz, $CDCl_3$, δ): 8.18 (d, J = 2.0 Hz, 1H), 7.80 (d, J = 8.0 Hz, 2H), 7.53 (dd, J = 8.8, 2.4 Hz, 1H), 7.34 (d, J = 8.4 Hz, 2H), 6.88 (d, J = 8.8 Hz, 2H), 6.77 (d, J = 8.8 Hz, 2H), 6.53 (d, J = 9.2 Hz, 1H), 4.86 (s, 2H), 4.26 (dd, J = 10.0, 3.2 Hz, 1H), 4.20−4.05 (m, 4H), 3.93 (dd, J = 9.2, 4.0 Hz, 1H), 3.10 (s, 6H), 2.43 (s, 3H), 1.41 (s, 3H), 1.38 (s, 3H). MS (ESI) (m/z): 543 [MH^+].

*(2,2-Dimethyl-5-(4-((6-(methylamino)pyridin-3-yl)-methoxy)phenoxy)-1,3-dioxolan-4-yl)methyl 4-methylbenzenesulfonate (**16**).* To a solution of **4** (138.2 mg, 1 mmol) and **14** (408.5 mg, 1 mmol) in THF (6 mL) was added triphenylphosphine (393.4 mg, 1.5 mmol), and then the mixture was cooled to 0 °C. Diisopropyl azodicarboxylate (303.3 mg, 1.5 mmol) in THF (3 mL) was added dropwisely at 0 °C, and then the reaction mixture was stirred at room temperature for 16 h. Evaporation of the solvent afforded a residue, which was purified by silica gel chromatography (AcOEt/hexane = 3/1) and aminopropyl silica gel chromatography (AcOEt/hexane = 1/1) to give 231.2 mg of **16** (43.7%). ^{1}H NMR (500 MHz, $CDCl_3$, δ): 8.12 (d, J = 2.0 Hz, 1H), 7.80 (d, J = 8.0 Hz, 2H), 7.52 (dd, J = 8.5, 2.0 Hz, 1H), 7.33 (d, J = 8.5 Hz, 2H), 6.88 (d, J = 9.0 Hz, 2H), 6.78 (d, J = 9.0 Hz, 2H), 6.41 (d, J = 8.5 Hz, 1H), 4.85 (s, 2H), 4.59 (s, 1H), 4.26 (dd, J = 10.5, 3.5 Hz, 1H), 4.20−4.06 (m, 4H), 3.93 (dd, J = 9.5, 4.5 Hz, 1H), 2.93 (d, J = 5.0 Hz, 3H), 2.43 (s, 3H), 1.41 (s, 3H), 1.38 (s, 3H). MS (ESI) (m/z): 529 [MH^+].

*5-((4-((5-(Fluoromethyl)-2,2-dimethyl-1,3-dioxolan-4-yl)-oxy)phenoxy)methyl)-N,N-dimethylpyridin-2-amine (**17**).* To a solution of **15** (271.3 mg, 0.5 mmol) in THF (7 mL) was added TBAF solution (1 M in THF, 2.0 mL). The reaction mixture was refluxed for 5.5 h. The solution was allowed to cool to room temperature and then extracted with AcOEt (60 mL × 2). The organic layers were combined and dried over Na_2SO_4. Evaporation of the solvent afforded a residue, which was purified by silica gel chromatography (AcOEt/hexane = 1/3) to give 69.2 mg of **17** (35.5%). ^{1}H NMR (500 MHz, $CDCl_3$, δ): 8.18 (d, J = 2.5 Hz, 1H), 7.52 (dd, J = 8.5, 2.5 Hz, 1H), 6.89 (d, J = 9.0 Hz, 2H), 6.84 (d, J = 9.0 Hz, 2H), 6.53 (d, J = 8.5 Hz, 1H), 4.86 (s, 2H), 4.71−4.50 (m, 2H), 4.28−4.13 (m, 3H), 4.01 (dd, J = 10.5, 3.5 Hz, 1H), 3.09 (s, 6H), 1.47 (s, 6H). MS (ESI) (m/z): 391 [MH^+].

*5-((4-((5-(Fluoromethyl)-2,2-dimethyl-1,3-dioxolan-4-yl)-oxy)phenoxy)methyl)-N-methylpyridin-2-amine (**18**).* To a solution of **16** (157.6 mg, 0.3 mmol) in THF (5 mL) was added TBAF solution (1 M in THF, 1.2 mL). The reaction mixture was refluxed for 4 h. The solution was allowed to cool to room temperature and then extracted with AcOEt (70 mL × 2). The organic layers were combined and dried over Na_2SO_4. Evaporation of the solvent afforded a residue, which was purified by silica gel chromatography (AcOEt/hexane = 1/1) to give 81.2 mg of **18** (72.4%). ^{1}H NMR (400 MHz, $CDCl_3$, δ): 8.12 (d, J = 2.4 Hz, 1H), 7.52 (dd, J = 8.8, 2.4 Hz, 1H), 6.89 (d, J = 8.8 Hz, 2H), 6.84 (d, J = 9.2 Hz, 2H), 6.41 (d, J = 8.8 Hz, 1H), 4.85 (s, 2H), 4.71−4.48 (m, 2H), 4.30−4.13 (m, 3H), 4.01 (dd, J = 9.2, 5.2 Hz, 1H), 2.93 (d, J = 5.2 Hz, 3H), 1.47 (s, 6H). MS (ESI) (m/z): 377 [MH^+].

*1-(4-((6-(Dimethylamino)pyridin-3-yl)methoxy)phenoxy)-4-fluorobutane-2,3-diol (**19**: FPMP-5).* To a solution of **17** (69.2 mg, 0.177 mmol) in MeOH (6 mL) was added 2 N HCl−MeOH (2.0 mL). The reaction mixture was stirred for 2.5 h at room temperature. The solution was quenched with sat. $NaHCO_3$ and 2 N NaOH at 0 °C and then extracted with AcOEt (20 mL × 2). The organic layers were combined and dried over Na_2SO_4. Evaporation of the solvent afforded a residue, which was purified by silica gel chromatography (AcOEt/hexane = 3/1) to give 38.5 mg of **19** (62.0%). ^{1}H NMR (400 MHz, $CDCl_3$, δ): 8.18 (d, J = 2.4 Hz, 1H), 7.52 (dd, J = 8.8, 2.4 Hz, 1H), 6.89 (d, J = 9.2 Hz, 2H), 6.84 (d, J = 9.2 Hz, 2H), 6.53 (d, J = 8.8 Hz, 1H), 4.86 (s, 2H), 4.66−4.47 (m, 2H), 4.08−4.03 (m, 4H), 3.10 (s, 6H), 2.63 (br, 2H). HRMS (FAB+) (m/z): [MH^+] calcd for $C_{18}H_{24}FN_2O_4$, 351.1720; found 351.1718.

*1-Fluoro-4-(4-((6-(methylamino)pyridin-3-yl)methoxy)-phenoxy)butane-2,3-diol (**20**: FPMP-6).* To a solution of **18** (77.8 mg, 0.207 mmol) in MeOH (6 mL) was added 2 N HCl−MeOH (2.5 mL). The reaction mixture was stirred for 3 h at room temperature. The solution was quenched with sat. $NaHCO_3$ and 2 N NaOH at 0 °C and then extracted with AcOEt (30 mL × 2). The organic layers were combined and dried over Na_2SO_4. Evaporation of the solvent afforded a residue, which was purified by silica gel chromatography ($CHCl_3$/MeOH = 10/1) to give 53.3 mg of **20** (76.7%). ^{1}H NMR (400 MHz, DMSO-d_6, δ): 8.02 (d, J = 2.4 Hz, 1H), 7.43 (dd, J = 8.4, 2.0 Hz, 1H), 6.91 (d, J = 9.2 Hz, 2H), 6.85 (d, J = 9.2 Hz, 2H), 6.55 (dd, J = 9.6, 4.4 Hz, 1H), 6.43 (d, J = 8.4 Hz, 1H), 5.13−5.05 (m, 2H), 4.09 (s 2H), 4.58−4.31 (m, 2H), 4.01−3.96 (m, 1H), 3.83−3.80 (m, 3H), 2.75 (d, J = 4.8 Hz, 3H). HRMS (FAB+) (m/z): [MH^+] calcd for $C_{17}H_{22}FN_2O_4$, 337.1564; found 337.1563.

Radiolabeling with ^{18}F. We produced [^{18}F]fluoride according to our method reported previously.[33] Kryptofix222 (10 mg) was dissolved in the solution of [^{18}F]fluoride in water. The solvent was removed at 120 °C under a stream of argon gas. The residue was azeotropically dried with 300 μL of anhydrous acetonitrile three times at 120 °C under a stream of nitrogen gas. To prepare [^{18}F]FPMP-1−4, a solution of the corresponding tosylate precursor (1.0 mg, purity: ≥ 95%) in acetonitrile (200 μL) was added to the reaction vessel containing the ^{18}F activity. The mixture was heated at 100 °C for 10 min. The ^{18}F-labeled compound was purified by HPLC on a COSMOSIL 5C_{18}-AR-II column with an isocratic solvent of acetonitrile/20 mM phosphate buffer, pH 7.0, at a flow rate of 1.0 mL/min ([^{18}F]FPMP-1 and [^{18}F]FPMP-3: acetonitrile/20 mM phosphate buffer, pH 7.0 = 40/60. [^{18}F]FPMP-2 and [^{18}F]FPMP-4: acetonitrile/20 mM phosphate buffer, pH 7.0 = 32/68.). To prepare [^{18}F]FPMP-5−6, a solution of the corresponding tosylate precursor (1.0 mg) in acetonitrile (200 μL) was added to the reaction vessel containing the ^{18}F activity. The mixture was heated at 100 °C for 10 min and subsequently cooled down. Then, 1 N HCl (100 μL) was added, and the mixture was heated at 100 °C again for 5 min. The solution was allowed to cool to room temperature, and then 300 μL of sat. $NaHCO_3$ aq. was added to adjust the pH. The mixture was extracted with ethyl acetate, and the solvent was evaporated under a stream of nitrogen gas. The residue was dissolved in the mobile phase (100 μL), and the solution was passed through a filter. The radiofluorinated ligand was purified by HPLC on a COSMOSIL 5C_{18}-AR-II column with an isocratic solvent of acetonitrile/20 mM phosphate buffer, pH 7.0, at a flow rate of 1.0 mL/min ([^{18}F]FPMP-5: acetonitrile/20 mM phosphate buffer, pH 7.0 = 28/72; [^{18}F]FPMP-6: acetonitrile/20 mM phosphate buffer,

DOI: 10.1021/acs.molpharmaceut.8b00756
Mol. Pharmaceutics XXXX, XXX, XXX−XXX

Scheme 1. Synthetic Route of FPMP-1−4

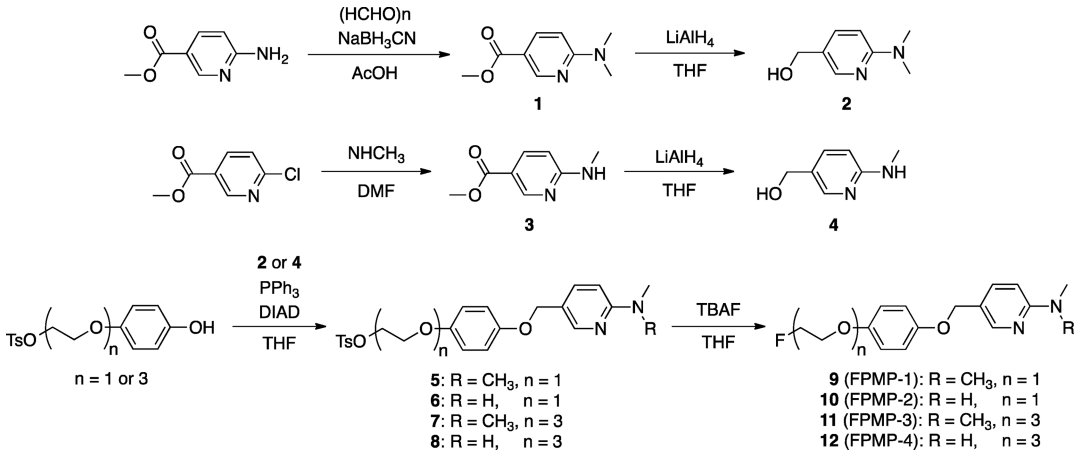

pH 7.0 = 20/80). The purity of all F-18 labeled compounds was determined by HPLC.

In Vitro Autoradiography Using Human Pancreas Sections. We performed in vitro autoradiography using human pancreas sections according to our method reported previously.[25] In this assay, the sections were incubated with ^{18}F-labeled PMP derivatives (370 kBq/1 μL) and were then washed with 10%EtOH (two 1 min washes) and rinsed with water (one 30-s wash).

ThS Staining of Islet Amyloids in Pancreas Sections. We performed ThS staining of islet amyloids in pancreas sections according to our method reported previously.[25]

Immunohistochemical Staining Using Human Pancreas Sections. We performed immunohistochemical staining using human pancreas sections according to our method reported previously.[25] In this study, the sections were autoclaved for 20 min in target retrieval solution (Agilent Technologies, Santa Clara, CA, USA) for antigen retrieval.

Animals. Animal experiments were conducted in accordance with our institutional guidelines and were approved by the Kyoto University Animal Care Committee. Male ddY mice were purchased from Japan SLC, Inc. (Shizuoka, Japan). ddY mice were fed standard chow and had free access to water. FVB/N-Tg(Ins2-IAPP)RHFSoel/J, wild-type FVB/NJ, and B6.C3-A^{vy}/J mice were purchased from The Jackson Laboratory (Bar Harbor, ME, USA). Wild-type C57BL/6J mice were purchased from Charles River (Yokohama, Japan). FVB/N-Tg(Ins2-IAPP)RHFSoel/J hemizygotes were bred with wild-type FVB/NJ mice to produce hemizygous hIAPP transgenic mice (hIAPP$^{Tg/o}$). FVB/N-Tg(Ins2-IAPP)-RHFSoel/J mice were crossed with B6.C3-A^{vy}/J mice to generate hIAPP$^{Tg/o}$ mice and wild-type littermate controls with A^{vy}/A at the agouti locus. These mice were fed a high-fat diet containing 45 kcal% fat (D12451, Research Diets, New Brunswick, NJ, USA) and had free access to water.

In Vivo Biodistribution in Normal Mice. We performed in vivo biodistribution in normal mice according to our method reported previously.[25] In this study, we used ^{18}F-labeled PMP derivatives (23.6−63.5 kBq in 100 μL).

Analysis of Radiometabolites in Blood and Pancreas. We performed analysis of radiometabolites in blood and pancreas according to our method reported previously.[34,35] In this study, we used [^{18}F]FPMP-5 (22.2−29.6 MBq in 150 μL), and the mice were sacrificed at 2, 30, and 60 min post-injection.

Ex Vivo Autoradiography Using Diabetes Model Mice. A saline solution (150 μL) of [^{18}F]FPMP-5 (74.0 MBq) containing EtOH (15 μL) was injected through the tail vein of hIAPP$^{Tg/o}$-A^{vy}/A mice (21 or 23 months-old, male, n = 2) and a WT-A^{vy}/A mouse (21 months-old, male, n = 1). The animals were sacrificed by decapitation at 60 min post-injection. The pancreas was immediately removed, embedded in super cryoembedding medium (SCEM) compound (SECTION-LAB Co., Ltd., Hiroshima, Japan), and then frozen in a dry ice/hexane bath. Frozen sections were prepared at a 20-μm thickness. The sections were exposed to a BAS imaging plate (Fuji Film) overnight. Autoradiographic images were obtained using a BAS5000 scanner system (Fuji Film). After autoradiographic examination, the adjacent sections were stained with ThS and an anti-amylin antibody to confirm the presence of islet amyloids.

Immunohistochemical Staining Using Pancreas Sections from Diabetes Model Mice. The sections were fixed in 4% paraformaldehyde in 0.1 M phosphate buffer (pH 7.4) for 30 min at room temperature, followed by two 3 min washes in PBS. They were then autoclaved for 20 min in target retrieval solution (Agilent Technologies) for antigen retrieval, followed by two 3 min incubations in PBS. The sections were incubated with MOM mouse IgG blocking reagent (Mouse on Mouse Elite Peroxidase kit, Vector Laboratories, Burlingame, CA, USA) for 1 h at room temperature, followed by two 2 min incubations in PBS. The sections were incubated with MOM diluent (Mouse on Mouse Elite Peroxidase kit, Vector Laboratories) for 5 min at room temperature, and then the excess of MOM diluent was removed. The sections were incubated with mouse monoclonal amylin primary antibody (1:200; R10/99, GeneTex, Inc., San Antonio, TX, USA), which is diluted with MOM diluent, for 30 min at room temperature. After two 2 min washes in PBS, they were incubated with biotinylated goat antimouse IgG (Mouse on Mouse Elite Peroxidase kit, Vector Laboratories) at room temperature for 10 min. After two 2 min washes in PBS, the sections were incubated with the streptavidin−peroxidase complex at room temperature for 5 min. After one 5 min incubation in PBS and one 5 min incubation in TBS, they were incubated with DAB as a chromogen for 5 min. After being washed with water, the sections were observed under a microscope (FSX100; Olympus).

DOI: 10.1021/acs.molpharmaceut.8b00756
Mol. Pharmaceutics XXXX, XXX, XXX−XXX

Scheme 2. Synthetic Route of FPMP-5−6

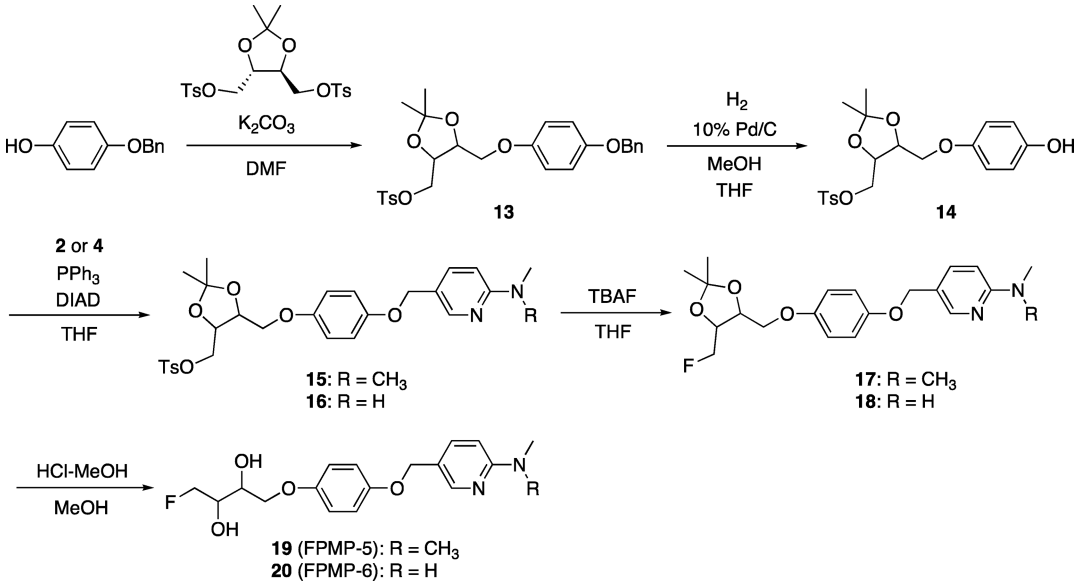

Scheme 3. ^{18}F Labeling of PMP Derivatives

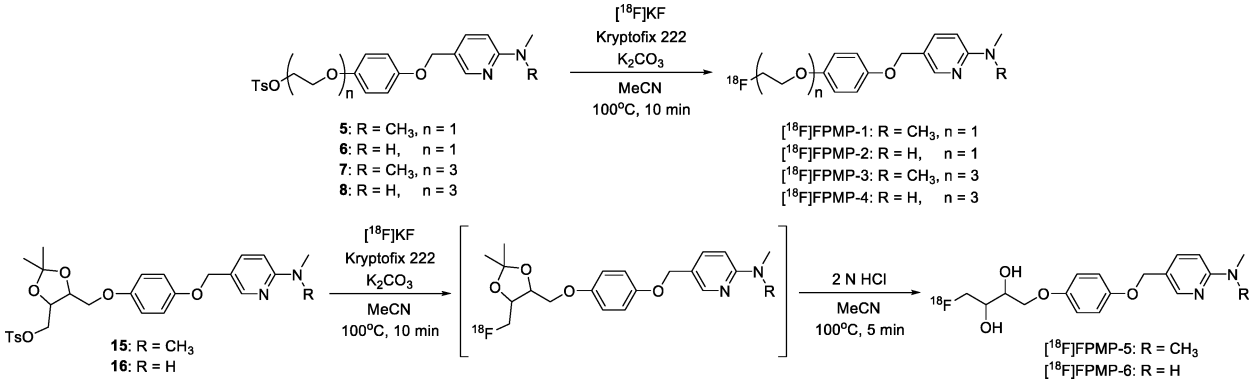

RESULTS AND DISCUSSION

Chemistry. The synthesis of nonradioactive FPMP-1−4 and FPMP-5−6 is shown in Schemes 1 and 2, respectively. The phenoxymethylpyridine backbone (**5**, **6**, **7**, **8**, **15**, and **16**) was obtained by the Mitsunobu reaction between the substituted phenols (2-(4-hydroxyphenoxy)ethyl 4-methylbenzenesulfonate, 2-(2-(2-(4-hydroxyphenoxy)ethoxy)ethoxy)-ethyl 4-methylbenzenesulfonate, and **14** and corresponding benzyl alcohols (**2** and **4**) in 21.6−62.6% yields. The fluorine derivatives (FPMP-1−4, **17**, and **18**) were obtained by refluxing the corresponding tosylate precursors (**5**, **6**, **7**, **8**, **15**, and **16**) with tetra-*n*-buthylammonium fluoride in anhydrous THF. Compounds **19** and **20** were subsequently deprotected of acetals to afford FPMP-5 and FPMP-6.

Radiolabeling. The desired radiofluorinated PMP derivatives were prepared from their corresponding tosylate precursors, as shown in Scheme 3. [^{18}F]FPMP-1, [^{18}F]FPMP-2, [^{18}F]FPMP-3, and [^{18}F]FPMP-4 were obtained via a nucleophilic displacement reaction with a [^{18}F]fluoride anion with radiochemical yields of 42.2, 34.3, 44.4, and 42.2%, respectively. To prepare [^{18}F]FPMP-5 and [^{18}F]FPMP-6, the corresponding precursors were reacted with [^{18}F]fluoride and then treated with aqueous HCl for the deprotection of acetals. Radiolabeling with ^{18}F was successfully performed on the precursor to generate [^{18}F]FPMP-5 and [^{18}F]FPMP-6 with radiochemical yields of 21.1 and 13.3%, respectively. Each radiolabeling was accomplished with a radiochemical purity greater than 95% with specific activity grater than 2.39 GBq/μmol. The radioactive PMP derivatives were identified by a comparison of the retention time with that of the non-radioactive compounds.

Autoradiography of Post-Mortem Pancreatic Sections with ^{18}F-Labeled PMP Derivatives. First, we tried to perform the competitive inhibition assay or the saturation binding assay to evaluate the binding affinity of FPMP derivatives. However, because FPMP derivatives weakly bind to synthetic amylin aggregates, it was difficult to compare the binding affinity of FPMP derivatives using these assays. A similar phenomenon was frequently reported in some papers describing the development of tau imaging probes. In these papers, the binding affinity of some tau imaging probes was evaluated with in vitro autoradiographic study using human brain sections, not with the binding assay using recombinant tau proteins.[34,36,37] Therefore, to evaluate the binding affinity for islet amyloids, in vitro autoradiographic studies with ^{18}F-labeled PMP derivatives were carried out using post-mortem human pancreatic sections. As shown in Figure 3, the autoradiographic images of each ^{18}F-labeled PMP derivative indicated their specific binding to islet amyloids. The pattern

DOI: 10.1021/acs.molpharmaceut.8b00756
Mol. Pharmaceutics XXXX, XXX, XXX−XXX

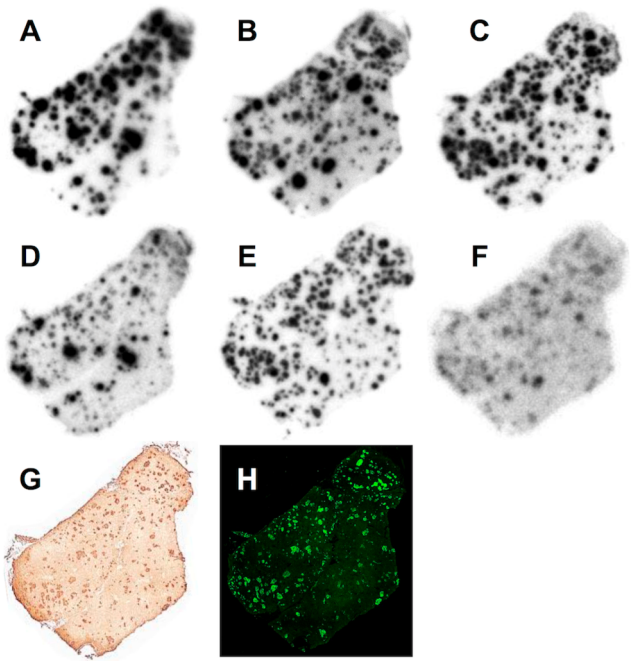

Figure 3. In vitro autoradiography of [^{18}F]FPMP-1 (A), [^{18}F]FPMP-2 (B), [^{18}F]FPMP-3 (C), [^{18}F]FPMP-4 (D), [^{18}F]FPMP-5 (E), and [^{18}F]FPMP-6 (F) with pancreatic sections from a T2DM patient. Adjacent sections were also stained with an antibody against amylin (G) and ThS (H).

of radioactivity accumulation was correlated with amylin immunostaining and thioflavin-S (ThS) staining in adjacent sections (Figures 2G and 2H, respectively). In contrast, no accumulation of radioactivity was observed on autoradiography using normal adult pancreas sections (Figures S2A–F), although a dense area was stained positively with amylin immunostaining (Figure S2G). ThS is a fluorescent dye commonly used for the detection of amyloid fibrils. Since there is no ThS labeling in normal pancreas sections (Figure S2H), they contained only natural amylin peptides stored in the pancreatic β-cells. Therefore, ^{18}F-labeled PMP derivatives displayed specific binding to amylin aggregates in islet amyloids, not to natural amylin peptides. The regions of interest (ROIs) were set in the T2DM pancreas section and healthy control pancreas section in the autoradiographic images, and intensity (PSL/mm^2) in each region was calculated for each probe. Then, we calculated the T2DM/healthy control ratio and compared the binding affinity for amylin aggregates between FPMP derivatives (Figure S3). This result showed that the dimethylamino derivatives ([^{18}F]FPMP-1, [^{18}F]FPMP-3, and [^{18}F]FPMP-5) have a higher binding affinity than the monomethylamino derivatives ([^{18}F]FPMP-2, [^{18}F]FPMP-4, and [^{18}F]FPMP-6). Taken together, [^{18}F]FPMP-1, [^{18}F]FPMP-3, and [^{18}F]FPMP-5 showed a sufficient potential to function as amylin imaging probes.

In Vivo Biodistribution in Normal Mice. Important requirements for amylin imaging agents involve the in vivo biodistribution characteristics, such as avoidance of accumulation in organs located near the pancreas and high uptake by the pancreas. Since the off-target accumulation in organs located near the pancreas impairs the signal-noise ratio, it is a serious problem for amylin imaging in vivo. Especially, the liver is located very close to the pancreas. Moreover, many radiotracers generally accumulate in the liver since it plays a major role in drug metabolism. Therefore, we evaluated the liver accumulation of ^{18}F-labeled PMP derivatives using normal ddY mice (Figure 4A). The biodistribution experiment in mice revealed moderate accumulation in the liver (11.0–23.7%ID/g at 2 min). Our previous study demonstrated that [^{99m}Tc]**1**, which is a ^{99m}Tc-labeled PBF derivative developed as an amylin imaging probe, displayed initial intensive accumulation in the liver (62.1%ID/g at 2 min).[23] ^{18}F-labeled PMP derivatives showed much lower accumulation in the liver than [^{99m}Tc]**1**, which is highly desirable for amylin imaging probes. Since several imaging probes with a ^{99m}Tc-IDA core showed high uptake by the liver despite their low-to-moderate lipophilicity as shown in the previous reports,[29,30] the high [^{99m}Tc]**1** uptake by the liver may also be due to the characteristics of its chelate. Therefore, exchange into the ^{18}F-labeled hydrophilic linker could help reduce the accumulation in the liver.

The high initial uptake by the target organ, that is the pancreas, is essential for amylin imaging in vivo, and moreover, imaging probes also need to have fast washout kinetics from normal pancreatic tissues. Therefore, we also evaluated biodistribution kinetics in the pancreas of ^{18}F-labeled PMP derivatives using normal mice. As shown in Figure 4B and Tables S1–6, each PMP derivative exhibited high initial uptake by the pancreas (4.67–6.00%ID/g at 2 min) and fast washout kinetics from the healthy pancreas (0.68–2.72%ID/g at 60

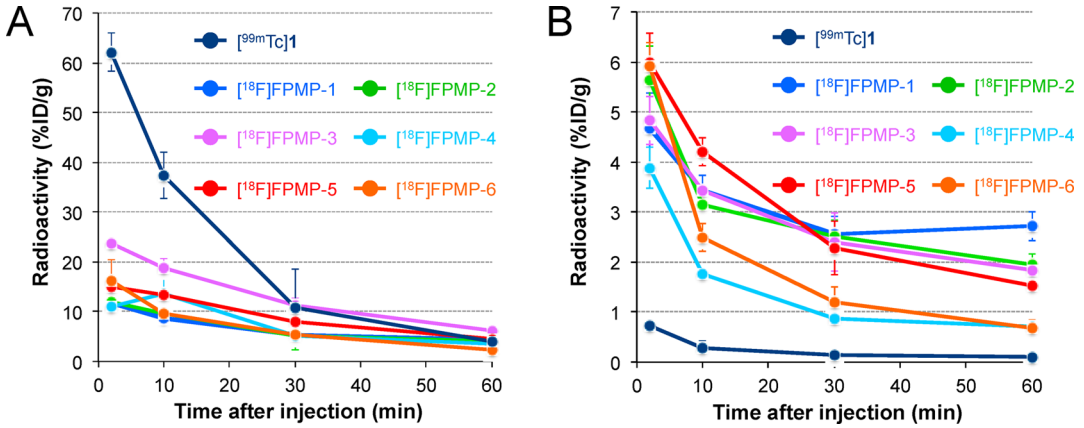

Figure 4. Comparison of liver (A) and pancreas (B) uptakes of radioactivity after injection of [^{18}F]FPMP-1–6 and [^{99m}Tc]**1** into normal ddY mice (male, n = 5). The data on [^{99m}Tc]**1** are reprinted from ref 25.

DOI: 10.1021/acs.molpharmaceut.8b00756
Mol. Pharmaceutics XXXX, XXX, XXX–XXX

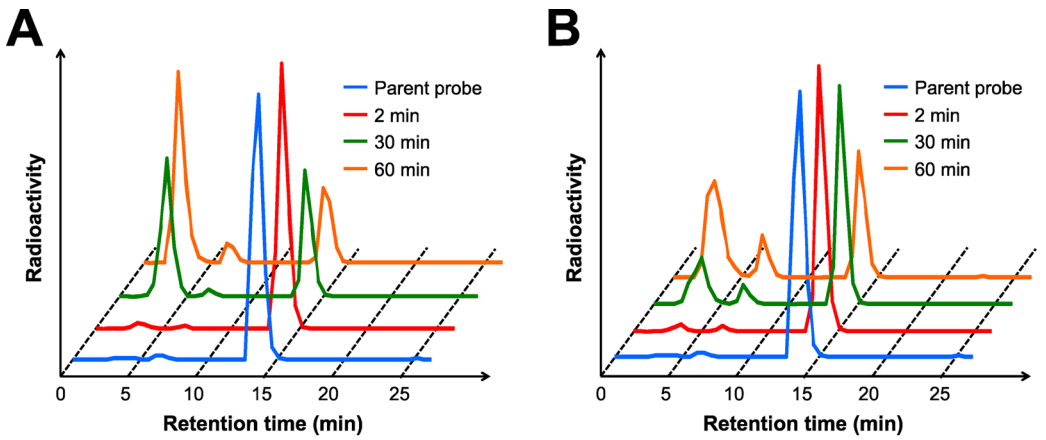

Time after injection (min)	Percentage of intact [^{18}F]FPMP-5
2	93.1 ± 3.4
30	41.8 ± 18.0
60	27.5 ± 5.6

Time after injection (min)	Percentage of intact [^{18}F]FPMP-5
2	93.7 ± 1.6
30	60.8 ± 18.6
60	36.3 ± 10.4

Figure 5. HPLC analysis of radiometabolites in the blood (A) and the pancreas (B) after injection of [^{18}F]FPMP-5 into normal ddY mice (male, n = 3−5).

min). Especially, [^{18}F]FPMP-5 and [^{18}F]FPMP-6 showed excellent initial uptake by the pancreas (6.00 and 5.92%ID/g at 2 min, respectively). According to our previous report, [^{99m}Tc] **1** displayed low initial uptake by the normal mouse pancreas (0.74%ID/g). We successfully developed novel radiolabeled tracers, which exhibited good in vivo kinetics, by reduction of the intensive exposure to the liver. Additionally, no marked uptake of ^{18}F-labeled PMP derivatives in bone was observed (1.23−4.89%ID/g at 60 min), indicating that they may show little defluorination in vivo, and interference with the imaging may be negligible (Tables S1−6). ^{18}F-labeled PMP derivatives exhibited low initial uptake by the stomach (2.62−3.91%ID at 2 min), but the accumulation of [^{18}F]FPMP-2, [^{18}F]FPMP-3, and [^{18}F]FPMP-5 in the stomach increased with time (11.3−15.7%ID/g at 60 min). Because the stomach is also located near the pancreas, this pharmacokinetics may be unfavorable for amylin imaging. Therefore, further improvement of the stomach uptake should be necessary to develop more useful probes for amylin imaging. In general, the chirality may influence the biological activities, including pharmacokinetics and metabolism.[38−41] Because there are two chiral carbons in FPMP-5 and FPMP-6, separation of optical isomers may improve the performance as the amylin imaging probe.

In Vivo Metabolic Stability of [^{18}F]FPMP-5. Considering the results of the binding to islet amyloid together with the biodistribution studies, we selected [^{18}F]FPMP-5 for further biological evaluations. We determined the in vivo metabolic stability of [^{18}F]FPMP-5 in normal ddY mice (Figure 5). After the injection of [^{18}F]FPMP-5 into ddY mice, the radiometabolites in the pancreas and blood were analyzed by HPLC. When radioactivity in mouse plasma was analyzed by HPLC, we confirmed the conversion of [^{18}F]FPMP-5 to several different chemical forms (Figure 5A). The percent of the intact form sequentially decreased and reached 93.1, 41.8, and 27.5% at 2, 30, and 60 min after injection, respectively (Figure 5A). When radioactivity in mouse pancreas was analyzed by HPLC, we identified a metabolic profile in the pancreas similar to that in the blood, suggesting that [^{18}F]FPMP-5 is rarely metabolized in the pancreas (Figure 5B). The percent of the intact form sequentially decreased and reached 93.7, 60.8, and 36.3% at 2, 30, and 60 min after injection, respectively (Figure 5B).

Ex Vivo Autoradiography of [^{18}F]FPMP-5 Using Transgenic Mice Expressing Human Amylin. To assess the binding ability of [^{18}F]FPMP-5 for islet amyloid in vivo, ex vivo autoradiography studies were carried out using an obese transgenic mouse model of T2DM expressing human amylin (hIAPP) under the rat insulin promoter in addition to the dominant agouti viable yellow mutation (A^{vy}), called the hIAPP$^{Tg/o}$-A^{vy}/A mouse. We also carried out the same experiments using a control mouse with A^{vy}/A, called the WT-A^{vy}/A mouse. In the male hIAPP$^{Tg/o}$-A^{vy}/A mouse, the progressive development of diabetes was observed by 15 weeks of age, and the islet amyloid was clearly present by 4 months of age and was more extensive by 10 months.[31,32] We conducted ex vivo autoradiography studies using 21-month-old male hIAPP$^{Tg/o}$-A^{vy}/A and WT-A^{vy}/A mice (Figure 6). Ex vivo autoradiograms after the injection of [^{18}F]FPMP-5 into a hIAPP$^{Tg/o}$-A^{vy}/A mouse showed the dense accumulation of islet amyloids in the pancreas (Figure 6A). The radioactivity in the pancreas showed an association with the signals obtained with ThS staining and amylin immunostaining using the adjacent pancreatic sections (Figure 6E,F,G). Conversely, no such [^{18}F]FPMP-5 labeling was observed in the WT-A^{vy}/A mouse pancreas (Figure 6C). Since the WT-A^{vy}/A mouse pancreas section showed no ThS staining (Figure 6D), [^{18}F]FPMP-5 may not bind to the normal pancreatic tissue. This was consistent with fast washout kinetics from the healthy pancreas in the biodistribution experiments (Figure 4B) and low nonspecific binding to the pancreas tissue from a healthy adult (Figure S2E).

DOI: 10.1021/acs.molpharmaceut.8b00756
Mol. Pharmaceutics XXXX, XXX, XXX−XXX

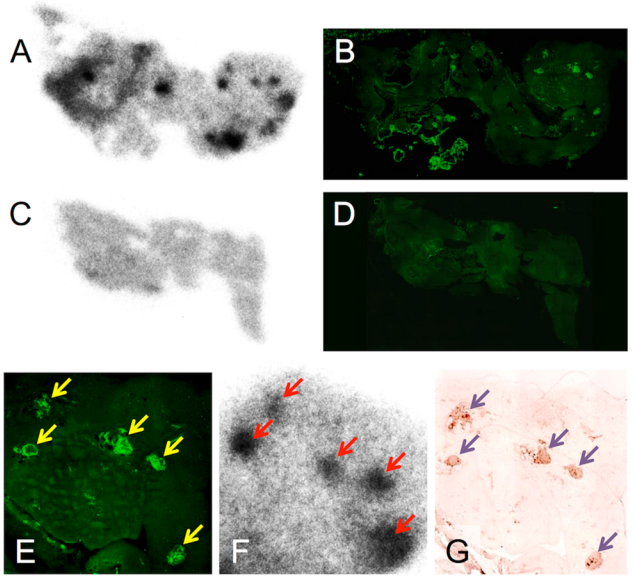

Figure 6. Ex vivo autoradiography with hIAPP$^{Tg/o}$-A^{vy}/A and WT-A^{vy}/A mice (male, 21 months old). Autoradiograms of [^{18}F]FPMP-5 using hIAPP^{Tg}-A^{vy}/A and WT-A^{vy}/A mice (A and C, respectively). ThS staining with the adjacent pancreatic sections (B and D, respectively). High magnification images of A and B (E and F, respectively). Amylin immunohistochemical staining with an adjacent pancreatic section (G).

CONCLUSIONS

In the present research, we designed and synthesized six novel ^{18}F-labeled PMP derivatives as amylin imaging probes in the T2DM pancreas. Each derivative showed affinity for islet amyloids in the T2DM pancreatic sections and good pharmacokinetics in normal mice. Among them, [^{18}F]FPMP-5 displayed not only clear labeling of islet amyloids but also the highest uptake by the mouse pancreas. In addition, ex vivo autoradiographic studies with [^{18}F]FPMP-5 revealed the intense labeling of islet amyloids in the pancreas of the diabetes model mouse in vivo. Taken together, [^{18}F]FPMP-5 has the feasibility as the amylin imaging probe to understand the T2DM pathology focusing on islet amyloid.

ASSOCIATED CONTENT

Supporting Information

The Supporting Information is available free of charge on the ACS Publications website at DOI: 10.1021/acs.molpharmaceut.8b00756.

In vivo biodistribution of [^{18}F]FPMP-1−6 in normal mice, representative HPLC profiles of nonradioactive and radioactive FPMP-1−6, in vitro autoradiography using pancreatic sections from a healthy adult, and ratio of radioactivity accumulation in the T2DM pancreas section against a healthy control pancreas section (PDF)

AUTHOR INFORMATION

Corresponding Author

*Phone +81-75-753-4556; Fax: +81-75-753-4568; E-mail: ono@pharm.kyoto-u.ac.jp.

ORCID

Masahiro Ono: 0000-0002-2497-039X

Hideo Saji: 0000-0002-3077-9321

Author Contributions

H.W. and M.Y. contributed to this work equally. H.W., M.Y., M.O., and H.S. designed the study. H.W. and M.Y. performed the experiments. H.W., M.Y., S.K., M.O., and H.S. analyzed the data. H.W., M.Y., and M.O. wrote the manuscript. All authors contributed to discussions and manuscript review. All authors have given approval for the final version of the manuscript.

Notes

The authors declare no competing financial interest.

ACKNOWLEDGMENTS

This work was supported by a grant from the Japan Society for the Promotion of Science (JSPS) through the "Funding Program for Next Generation World-Leading Researchers (LS060)", initiated by the Council for Science and Technology Policy (CSTP), and JSPS Research Fellowships for Young Scientists (14J05961).

ABBREVIATIONS

T2DM, type 2 diabetes mellitus; BCM, β-cell mass; IAPP, islet amyloid polypeptide; Aβ, β-amyloid; PET, positron emission tomography; IDA, iminodiacetic acid; ThS, thioflavin-S; PBS, phosphate-buffered saline; TBS, tris-buffered saline; DAB, 3,3′-diaminobenzidine; THF, tetrahydrofuran; DMF, *N*,*N*-dimethylformamide; (HCHO)n, paraformaldehyde; MeCN, acetonitrile; DIAD, diisopropyl azodicarboxylate; TBAF, tetra-*n*-butylammonium fluoride; AcOEt, ethyl acetate; NMR, nuclear magnetic resonance; MS (ESI or APCI), mass spectrometry (electrospray ionization or atmospheric pressure chemical ionization); HRMS (FAB), high-resolution mass spectrometry (fast atom bombardment); TMS, tetramethylsilane; *J*, coupling constant (in NMR spectrometry); HPLC, high-performance liquid chromatography.

REFERENCES

(1) American Diabetes Association. Diagnosis and classification of diabetes mellitus. *Diabetes Care* **2014**, *37*, S81−S90.

(2) Bardenheier, B. H.; Lin, J.; Zhuo, X.; Ali, M. K.; Thompson, T. J.; Cheng, Y. J.; Gregg, E. W. Disability-Free Life-Years Lost Among Adults Aged ≥ 50 Years With and Without Diabetes. *Diabetes Care* **2016**, *39* (7), 1222−9.

(3) World Health Organization. World health organization diabetes fact sheet #32. www.who.int/mediacentre/factsheets/fs312/en, (accessed Jan 2015).

(4) Guariguata, L.; Whiting, D. R.; Hambleton, I.; Beagley, J.; Linnenkamp, U.; Shaw, J. E. Global estimates of diabetes prevalence for 2013 and projections for 2035. *Diabetes Res. Clin. Pract.* **2014**, *103* (2), 137−49.

(5) Herman, W. H.; Fajans, S. S. Hemoglobin A1c for the diagnosis of diabetes: practical considerations. *Polym. Arch. Med. Wewn.* **2010**, *120* (1−2), 37−40.

(6) Sacks, D. B. A1C versus glucose testing: a comparison. *Diabetes Care* **2011**, *34* (2), 518−23.

(7) Inzucchi, S. E. Clinical practice. Diagnosis of diabetes. *N. Engl. J. Med.* **2012**, *367* (6), 542−50.

(8) Stancakova, A.; Javorsky, M.; Kuulasmaa, T.; Haffner, S. M.; Kuusisto, J.; Laakso, M. Changes in insulin sensitivity and insulin release in relation to glycemia and glucose tolerance in 6,414 Finnish men. *Diabetes* **2009**, *58* (5), 1212−21.

(9) Butler, A. E.; Janson, J.; Bonner-Weir, S.; Ritzel, R.; Rizza, R. A.; Butler, P. C. β-cell deficit and increased β-cell apoptosis in humans with type 2 diabetes. *Diabetes* **2003**, *52* (1), 102−10.

(10) de Koning, E. J.; Bonner-Weir, S.; Rabelink, T. J. Preservation of β-cell function by targeting β-cell mass. *Trends Pharmacol. Sci.* **2008**, *29* (4), 218−27.

DOI: 10.1021/acs.molpharmaceut.8b00756
Mol. Pharmaceutics XXXX, XXX, XXX−XXX

(11) Rahier, J.; Guiot, Y.; Goebbels, R. M.; Sempoux, C.; Henquin, J. C. Pancreatic β-cell mass in European subjects with type 2 diabetes. *Diabetes, Obes. Metab.* **2008**, *10*, 32−42.
(12) Fagerholm, V.; Mikkola, K. K.; Ishizu, T.; Arponen, E.; Kauhanen, S.; Nagren, K.; Solin, O.; Nuutila, P.; Haaparanta, M. Assessment of islet specificity of dihydrotetrabenazine radiotracer binding in rat pancreas and human pancreas. *J. Nucl. Med.* **2010**, *51* (9), 1439−46.
(13) Kung, M. P.; Hou, C.; Lieberman, B. P.; Oya, S.; Ponde, D. E.; Blankemeyer, E.; Skovronsky, D.; Kilbourn, M. R.; Kung, H. F. In vivo imaging of β-cell mass in rats using ^{18}F-FP-(+)-DTBZ: a potential PET ligand for studying diabetes mellitus. *J. Nucl. Med.* **2008**, *49* (7), 1171−6.
(14) Clark, P. B.; Gage, H. D.; Brown-Proctor, C.; Buchheimer, N.; Calles-Escandon, J.; Mach, R. H.; Morton, K. A. Neurofunctional imaging of the pancreas utilizing the cholinergic PET radioligand [^{18}F]4-fluorobenzyltrozamicol. *Eur. J. Nucl. Med. Mol. Imaging* **2004**, *31* (2), 258−60.
(15) Hubalewska-Dydejczyk, A.; Sowa-Staszczak, A.; Tomaszuk, M.; Stefanska, A. GLP-1 and exendin-4 for imaging endocrine pancreas. A review. Labelled glucagon-like peptide-1 analogues: past, present and future. *Q. J. Nucl. Med. Mol. Imaging* **2015**, *59* (2), 152−160.
(16) Weir, G. C.; Laybutt, D. R.; Kaneto, H.; Bonner-Weir, S.; Sharma, A. β-cell adaptation and decompensation during the progression of diabetes. *Diabetes* **2001**, *50*, S154−S159.
(17) Weir, G. C.; Bonner-Weir, S. Five stages of evolving β-cell dysfunction during progression to diabetes. *Diabetes* **2004**, *53*, S16−S21.
(18) Khadra, A.; Schnell, S. Development, growth and maintenance of β-cell mass: models are also part of the story. *Mol. Aspects Med.* **2015**, *42*, 78−90.
(19) Hoppener, J. W.; Ahren, B.; Lips, C. J. Islet amyloid and type 2 diabetes mellitus. *N. Engl. J. Med.* **2000**, *343* (6), 411−9.
(20) Abedini, A.; Schmidt, A. M. Mechanisms of islet amyloidosis toxicity in type 2 diabetes. *FEBS Lett.* **2013**, *587* (8), 1119−27.
(21) Marzban, L.; Park, K.; Verchere, C. B. Islet amyloid polypeptide and type 2 diabetes. *Exp. Gerontol.* **2003**, *38* (4), 347−351.
(22) Yoshimura, M.; Ono, M.; Watanabe, H.; Kimura, H.; Saji, H. Feasibility of amylin imaging in pancreatic islets with β-amyloid imaging probes. *Sci. Rep.* **2015**, *4*, 6155.
(23) Lu, Z.; Xie, J.; Yan, R.; Yu, Z.; Sun, Z.; Yu, F.; Gong, X.; Feng, H.; Lu, J.; Zhang, Y. A pilot study of pancreatic islet amyloid PET imaging with [^{18}F]FDDNP. *Nucl. Med. Commun.* **2018**, *39* (7), 659−64.
(24) Templin, A. T.; Meier, D. T.; Willard, J. R.; Wolden-Hanson, T.; Conway, K.; Lin, Y. G.; Gillespie, P. J.; Bokvist, K. B.; Attardo, G.; Kahn, S. E.; Scheuner, D.; Hull, R. L. Use of the PET ligand florbetapir for in vivo imaging of pancreatic islet amyloid deposits in hIAPP transgenic mice. *Diabetologia* **2018**, *61* (10), 2215−24.
(25) Yoshimura, M.; Ono, M.; Watanabe, H.; Kimura, H.; Saji, H. Development of ^{99m}Tc-Labeled Pyridyl Benzofuran Derivatives To Detect Pancreatic Amylin in Islet Amyloid Model Mice. *Bioconjugate Chem.* **2016**, *27* (6), 1532−9.
(26) Yang, Y.; Cui, M.; Zhang, X.; Dai, J.; Zhang, Z.; Lin, C.; Guo, Y.; Liu, B. Radioiodinated benzyloxybenzene derivatives: a class of flexible ligands target to β-amyloid plaques in Alzheimer's brains. *J. Med. Chem.* **2014**, *57* (14), 6030−42.
(27) Yang, Y.; Zhang, X.; Cui, M.; Zhang, J.; Guo, Z.; Li, Y.; Zhang, X.; Dai, J.; Liu, B. Preliminary Characterization and In Vivo Studies of Structurally Identical ^{18}F- and ^{125}I-Labeled Benzyloxybenzenes for PET/SPECT Imaging of β-Amyloid Plaques. *Sci. Rep.* **2015**, *5*, 12084.
(28) Yang, Y.; Fu, H.; Cui, M.; Peng, C.; Liang, Z.; Dai, J.; Zhang, Z.; Lin, C.; Liu, B. Preliminary evaluation of fluoro-pegylated benzyloxybenzenes for quantification of β-amyloid plaques by positron emission tomography. *Eur. J. Med. Chem.* **2015**, *104*, 86−96.
(29) Djokic, D. D.; Jankovic, D. L.; Stamenkovic, L. L.; Pirmettis, I. Chemical and biological evaluation of ^{99m}Tc(CO)$_3$ and ^{99m}Tc complexes of some IDA derivatives. *J. Radioanal. Nucl. Chem.* **2004**, *260* (3), 471−76.
(30) Serdons, K.; Verduyckt, T.; Cleynhens, J.; Bormans, G.; Verbruggen, A. Development of ^{99m}Tc-thioflavin-T derivatives for detection of systemic amyloidosis. *J. Labelled Compd. Radiopharm.* **2008**, *51* (10), 357−67.
(31) Soeller, W. C.; Janson, J.; Hart, S. E.; Parker, J. C.; Carty, M. D.; Stevenson, R. W.; Kreutter, D. K.; Butler, P. C. Islet amyloid-associated diabetes in obese A(vy)/a mice expressing human islet amyloid polypeptide. *Diabetes* **1998**, *47* (5), 743−50.
(32) Butler, A. E.; Janson, J.; Soeller, W. C.; Butler, P. C. Increased β-cell apoptosis prevents adaptive increase in β-cell mass in mouse model of type 2 diabetes: evidence for role of islet amyloid formation rather than direct action of amyloid. *Diabetes* **2003**, *52* (9), 2304−14.
(33) Ono, M.; Cheng, Y.; Kimura, H.; Cui, M.; Kagawa, S.; Nishii, R.; Saji, H. Novel ^{18}F-labeled benzofuran derivatives with improved properties for positron emission tomography (PET) imaging of beta-amyloid plaques in Alzheimer's brains. *J. Med. Chem.* **2011**, *54* (8), 2971−9.
(34) Matsumura, K.; Ono, M.; Kitada, A.; Watanabe, H.; Yoshimura, M.; Iikuni, S.; Kimura, H.; Okamoto, Y.; Ihara, M.; Saji, H. Structure-Activity Relationship Study of Heterocyclic Phenylethenyl and Pyridinylethenyl Derivatives as Tau-Imaging Agents That Selectively Detect Neurofibrillary Tangles in Alzheimer's Disease Brains. *J. Med. Chem.* **2015**, *58* (18), 7241−57.
(35) Ono, M.; Watanabe, H.; Kitada, A.; Matsumura, K.; Ihara, M.; Saji, H. Highly Selective Tau-SPECT Imaging Probes for Detection of Neurofibrillary Tangles in Alzheimer's Disease. *Sci. Rep.* **2016**, *6*, 34197.
(36) Maruyama, M.; Shimada, H.; Suhara, T.; Shinotoh, H.; Ji, B.; Maeda, J.; Zhang, M. R.; Trojanowski, J. Q.; Lee, V. M.; Ono, M.; Masamoto, K.; Takano, H.; Sahara, N.; Iwata, N.; Okamura, N.; Furumoto, S.; Kudo, Y.; Chang, Q.; Saido, T. C.; Takashima, A.; Lewis, J.; Jang, M. K.; Aoki, I.; Ito, H.; Higuchi, M. Imaging of tau pathology in a tauopathy mouse model and in Alzheimer patients compared to normal controls. *Neuron* **2013**, *79* (6), 1094−108.
(37) Xia, C. F.; Arteaga, J.; Chen, G.; Gangadharmath, U.; Gomez, L. F.; Kasi, D.; Lam, C.; Liang, Q.; Liu, C.; Mocharla, V. P.; Mu, F.; Sinha, A.; Su, H.; Szardenings, A. K.; Walsh, J. C.; Wang, E.; Yu, C.; Zhang, W.; Zhao, T.; Kolb, H. C. [^{18}F]T807, a novel tau positron emission tomography imaging agent for Alzheimer's disease. *Alzheimer's Dementia* **2013**, *9* (6), 666−76.
(38) Brocks, D. R. Drug disposition in three dimensions: an update on stereoselectivity in pharmacokinetics. *Biopharm. Drug Dispos.* **2006**, *27* (8), 387−406.
(39) Tago, T.; Furumoto, S.; Okamura, N.; Harada, R.; Adachi, H.; Ishikawa, Y.; Yanai, K.; Iwata, R.; Kudo, Y. Preclinical Evaluation of [^{18}F]THK-5105 Enantiomers: Effects of Chirality on Its Effectiveness as a Tau Imaging Radiotracer. *Mol. Imaging Biol.* **2016**, *18* (2), 258−66.
(40) Yang, Y.; Wang, X.; Yang, H.; Fu, H.; Zhang, J.; Zhang, X.; Dai, J.; Zhang, Z.; Lin, C.; Guo, Y.; Cui, M. Synthesis and Monkey-PET Study of (R)- and (S)-^{18}F-Labeled 2-Arylbenzoheterocyclic Derivatives as Amyloid Probes with Distinctive in Vivo Kinetics. *Mol. Pharmaceutics* **2016**, *13* (11), 3852−63.
(41) Tago, T.; Furumoto, S.; Okamura, N.; Harada, R.; Adachi, H.; Ishikawa, Y.; Yanai, K.; Iwata, R.; Kudo, Y. Structure-Activity Relationship of 2-Arylquinolines as PET Imaging Tracers for Tau Pathology in Alzheimer Disease. *J. Nucl. Med.* **2016**, *57* (4), 608−14.

DOI: 10.1021/acs.molpharmaceut.8b00756
Mol. Pharmaceutics XXXX, XXX, XXX−XXX